Photoemission study of K on graphite

P. Bennich, C. Puglia, P. A. Brühwiler, A. Nilsson, A. J. Maxwell, A. Sandell, and N. Mårtensson
Department of Physics, Uppsala University, Box 530, S-751 21 Uppsala, Sweden

P. Rudolf
LISE, Facultes Universitaires Notre-Dame de la Paix, Rue de Bruxelles 61, B-5000 Namur, Belgium
(Received 23 October 1998)

The physical and electronic structure of the dispersed and (2×2) phases of K/graphite have been characterized by valence and core-level photoemission. Charge transfer from K to graphite is found to occur at all coverages, and includes transfer of charge to the second graphite layer. A rigid band description is reasonably successful in describing important aspects of the data, and our results are consistent with a shift of approximately 0.4 eV in the surface graphite layer for both phases. The C 1*s* line shape and binding-energy shift as a function of charge transfer can be understood qualitatively by taking into account rigid band effects and the effects of a core hole on the density of states. For the (2×2) phase the metallic overlayer contributes extrinsic satellites to the C 1*s* line shape. The K 3*p* spectrum is strongly affected by the overlayer phase, and in addition indicates very little variation in the substrate charge distribution as a function of coverage in the dispersed phase. The lack of an interface K 3*p* binding-energy shift for a K bilayer or multilayer is ascribed to a weak K-graphite bond for metallic overlayers. The results have implications for the interpretation of photoelectron spectra of alkali graphite intercalation compounds (GIC's). [S0163-1829(99)09111-0]

I. INTRODUCTION

The characteristics of alkali metals adsorbed on metal substrates have been studied for a long time, mainly because the relatively simple electronic structure of the alkalis makes these systems attractive as simple models for chemisorption.[1] Despite the apparent simplicity, however, the nature of the alkali-substrate bond has been a long-standing question which is still under consideration (see, e.g., Ref. 2 and references therein).

A subclass of these studies concerns alkali adsorption on graphite. Graphite is a semimetal with very low density of states (DOS) around the Fermi level (E_F). It is often regarded as a prototypical layered crystal, since the interlayer distance (3.35 Å) is much larger than the intralayer C-C distance (1.42 Å). This is because the carbon 2*s* and 2*p* orbitals form in-plane sp^2 hybrids, which leads to strong, covalent σ bonds and out-of-plane lone-pair p_z hybrids which form delocalized intralayer and weak interlayer π bonds. Graphite thus has a pronounced two-dimensional electronic structure, which makes it a particularly interesting choice as a substrate in alkali adsorption studies. In addition, the ordered phase of K on the graphite basal plane is accessible to band-structure calculations.

Another motivation for the present work is the many studies of graphite intercalation compounds (GIC's):[3–5] If their mobility is sufficiently high, foreign atoms (intercalants) can move into the bulk and, in particular, form ordered structures between the graphite layers. Depending on the electronegativity of these atoms, it is common to divide the resulting compounds into acceptor (electronegative intercalants) and donor (electropositive intercalants) compounds, which refers to whether charge is withdrawn from or transferred to the graphite, respectively. The electronic properties of the graphite may change considerably due to the intercalants; it is for example found that the electric conductivity along the planes increases dramatically (see Ref. 6 and references therein). A key to understanding the GIC's lies in connecting structural and electronic properties, and one approach to this issue is to study the corresponding overlayer systems. It is also worth pointing out that similar electronic and structural aspects occur for the interesting alkali-C_{60} compounds, whose transport properties are often compared to those of intercalated graphite, and which, like the GIC's, are superconducting but at relatively higher temperatures (see, e.g., Ref. 7).

For the case of K/graphite, by means of a combination of one-dimensional low-energy electron diffraction (LEED) and electron energy loss spectroscopy (EELS), many details on the coverage-dependent behavior have been revealed:[8–11] low coverages can be prepared wherein the K atoms are partly ionized and distributed uniformly on the surface due to dipole-dipole interactions. With increasing coverage, the overlayer compresses *uniformly* until a critical coverage (Θ) of 0.1 monolayer (ML) is reached. Coverages below this limit will hereafter be referred to as a *dispersed phase*, whereas the critical coverage itself (0.1 ML) will be denoted a *saturated* (fully developed) dispersed phase. At 0.1 ML the potassium roughly forms a (7×7) overlayer.[8]

Above 0.1 ML, (2×2) islands start to nucleate, coexisting with and replacing the dispersed phase until the (2×2) overlayer is fully developed, i.e., a complete phase transformation takes place. The region between 0.1 and 1 ML will be referred to as a mixed phase. Previous LEED work[12] had identified the (2×2) phase, and also suggested that a $(\sqrt{3}\times\sqrt{3})R30°$ phase is formed at higher coverage. To our knowledge this last phase has not been confirmed in any other studies, and the (2×2) phase will be considered here as corresponding to $\Theta=1$ ML.

The temperature is a critical parameter in these experiments. For example, above 50 K the mobility of the K at-

oms in the dispersed phase has been shown high enough to cause intercalation.[11] On the other hand, lower temperatures (30 K) hinder adjustments to the dipole-dipole repulsion between the K atoms, which leads to nonuniform distributions.[8] In the case of multilayers, it was found that the overlayer intercalated at temperatures above approximately 150 K. No estimation of the critical temperature for intercalation was performed on the (2×2) phase in Ref. 11, however.

Apart from the geometrical information, electronic structure information was obtained[8,9] by monitoring electronic excitations at the different coverages. At coverages in the dispersed regime, a characteristic graphite surface charge carrier plasmon was seen, whose energy increased monotonically with coverage up to 0.1 ML. In the mixed-phase region (0.1–1 ML), the charge carrier plasmon energy was found to stay constant at 0.32 eV, whereas the *intensity* decreased until it vanished completely[9] at 1 ML. However, new electronic excitations appeared at 0.1 ML, with energies of 1.2,1.5, and 2.2 eV, which partly vanished[8] at 1 ML. At 1 ML a broad feature between approximately 0.5 and 1.2 eV was clearly seen, together with yet another feature at 2.7 eV.

The interpretation given for the evolution of electronic excitations noted above is in brief the following: the graphite surface charge carrier plasmon in the dispersed phase increases in energy because more and more charge is transferred from the K overlayer into the graphite. The 1.2, 1.5, and 2.2 eV EELS loss features in the mixed-phase region were attributed to atomiclike excitations in K atoms situated at the edges of (2×2) islands, which would explain their partial disappearance at 1 ML. No explanation for the broad feature between 0.5 and 1.2 eV at 1 ML coverage was given, however. Finally, the disappearance of the 0.32 eV plasmon at 1 ML was suggested to be due to the withdrawal of charge back to the K overlayer when forming the (2×2) phase.[8,10] This phase has metallic character, because the 2.7 eV plasmon can be interpreted as a metallic K surface plasmon, in accord with previous EELS studies of solid[13] K.

There are only a few photoemission studies of K/graphite, to our knowledge. In Refs. 14–16, both x-ray and angle-resolved ultraviolet photoemission (XPS and ARUPS, respectively) were applied to the C $1s$ and K $2p$ levels and the valence bands. No trace of a metallic K $4s$ band in the (2×2) phase was seen in the XP valence spectra based on cross-section arguments. On the other hand, an enhancement below the Fermi level was seen in the UP spectra which was attributed to graphite π bands. These results thus indicated a complete charge transfer to the graphite in the (2×2) phase, in contradiction to the EELS results reviewed above. The temperature in the photoemission experiments was 110 K, however, at which intercalation would have occurred to a significant extent.

In this paper, we present photoemission results for K/graphite with coverages ranging from the dispersed phase regime to the (2×2) phase. The effects on both the potassium and the graphite have been traced by measuring the C $1s$, K $3p$, and valence levels. The motivation is mainly to investigate the discrepancies among the experiments already mentioned, and to reveal new aspects of the influence of potassium on graphite. We will also compare our conclusions for this system with previous results obtained for potassium-based GIC's, and discuss possible alternative explanations for the relevant work in that area, taking advantage of the present well-characterized surface.

A central issue in our discussion of the results is the so-called ''rigid band model.'' This is a simple model in which the interaction between graphite and an adsorbate or intercalant is limited to charge donation or removal by the atom, without other influences on the graphite bands, i.e., there is a type of idealized ionic bond. For example, if electropositive atoms such as the alkalis were to be placed on the graphite surface, it would be assumed that they would donate a fraction of their charge into the empty density of states (DOS) above E_F. Since the DOS is so shallow, the position of E_F in the DOS will move substantially upwards due to the charge transfer, even when the total amount of the donated charge is small. The model thus offers a way to understand observed binding-energy shifts, estimate the amount of transferred charge, etc., and is therefore often discussed in studies on GIC's[2,17–19] and alkali/graphite[10,15] systems. However, the nature of the alkali-substrate bond is still under debate,[2] as is the alkali-graphite bonding in GIC's,[20] where especially the question of where the charge actually resides is still an open one. Therefore, we employ the rigid band model as an approximation which is attractive because of its simplicity and easy applicability. Our approach is described in more detail at the end of Sec. III A 2.

II. EXPERIMENT

Photelectron spectroscopy (PES) measurements of the C $1s$ and K $3p$ levels, as well as of the graphite valence band, were performed at Max I, the Swedish synchrotron radiation facility in Lund, using a modified SX-700 monochromator and a hemispherical analyzer of Scienta type.[21] The sample preparation chamber had a base pressure of 1×10^{-10} Torr, and the measurement chamber had an operating pressure of $(7-8)\times10^{-11}$ Torr. The resolution was set to 0.2 eV for the K $3p$ spectra and 0.3 eV for the C $1s$ and valence spectra. All the data presented here were taken with the photons incident at 40° and electrons emitted at 0° with respect to the surface normal.

Separate measurements on the valence levels together with angle-resolved XPS measurements of the C $1s$ level were carried out in Uppsala. The experimental system consists of two interconnected UHV chambers, one for sample preparation and one housing the spectrometer. Both chambers had a base pressure of $(1-2)\times10^{-10}$ Torr. The spectrometer is based on a rotating anode yielding Al K_α radiation (1486.6 eV) and a hemispherical electron analyzer (mean radius 360 mm) together with a multichannel detector system.[22] A He gas discharge lamp was also used, providing He II_α radiation (40.8 eV). The resolution for the Al K_α valence spectra was 0.8 eV, whereas it was 0.4 eV for the He II_α valence spectra. Furthermore, it varied between 0.3 and 0.5 eV for the angle-resolved C $1s$ measurements.

The highly oriented pyrolytic graphite (HOPG) sample was mounted on a copper block, which was connected to the cold finger of a liquid He cryostat. The temperature was measured with a Chromel-Constantan thermocouple, and sample temperatures as low as 25 K could be achieved as confirmed by Ar adsorption/desorption. The graphite was

cleaned by resistive heating: a large current was forced to pass perpendicularly to the graphite planes to take advantage of the 100-times-larger resistance in this direction.[23] C 1*s* spectra were recorded to check for potassium residues since the binding energy and line shape of this level are extremely sensitive to whether potassium is present or not (see Sec. III C). O 1*s* spectra were also recorded to ensure that no oxygen was present.

K overlayers were prepared by evaporating potassium using a well-outgassed commercial getter source (SAES), while keeping the graphite substrate at 90 K. Immediately after reaching the desired coverage [dispersed or (2×2)], the sample was cooled down and thereafter held at 25 K. The elevated temperature during evaporation is necessary to obtain a mobility high enough to allow the single K atoms to spread out uniformly on the surface without forming (2×2) islands, while the lower post preparation temperature is necessary to avoid intercalation.[8] However, the probability for coadsorption of atoms or molecules (especially oxygen-containing species) from the residual gas at this temperature is non-negligible, and the overlayer was therefore checked regularly to avoid measurements on contaminated preparations. From elaborate growth studies it was found that the different phases are characterized by distinctive C 1*s*, K 3*p*, and valence spectra, and this was utilized when preparing the overlayer.

III. RESULTS

A. Valence band

1. Extended region; 0–30 eV

In this section we will discuss the different features observed in the valence photoemission data, and interpret differences between the phases in terms of modifications due to the overlayer, together with possible binding-energy shifts of the whole valence region. The shifts will be connected later to the discussion of observed binding-energy shifts for the C 1*s* level.

Figure 1 displays the valence band for clean graphite and for the dispersed and (2×2) phases. The spectrum for clean graphite has a characteristic appearance, dominated by the σ band centered at 21.2 eV and the π band centered at 7.5 eV. Furthermore, there is vanishing intensity at E_F in accordance with the semimetallic character of graphite. Turning next to the dispersed phase, we see that the shape of the σ band has changed somewhat and is slightly broader; this is caused by the K 3*p* level, which starts to appear in this energy region. The shape of the π band is, on the other hand, essentially unchanged, and a comparison with the π band in the clean spectrum reveals a shift of 0.4 eV towards higher binding energy.

Finally, in the (2×2) phase the σ and π bands are considerably broader, with an asymmetry to higher binding energy. The peak maxima are apparently shifted to 21.7 eV and 8.4 eV, respectively. A shoulder is visible at around 25 eV. Two new features appear at 18.5 and 1 eV, respectively, and a cutoff at E_F is now clearly seen. The 18.5 eV peak is the K 3*p* level, now fully developed, and will be discussed in detail in Sec. III B. The next section (Sec. III A 2) deals with the origin of the enhancement in the vicinity of the Fermi level. The rest of this section will focus on the shape of the valence band for the (2×2) phase.

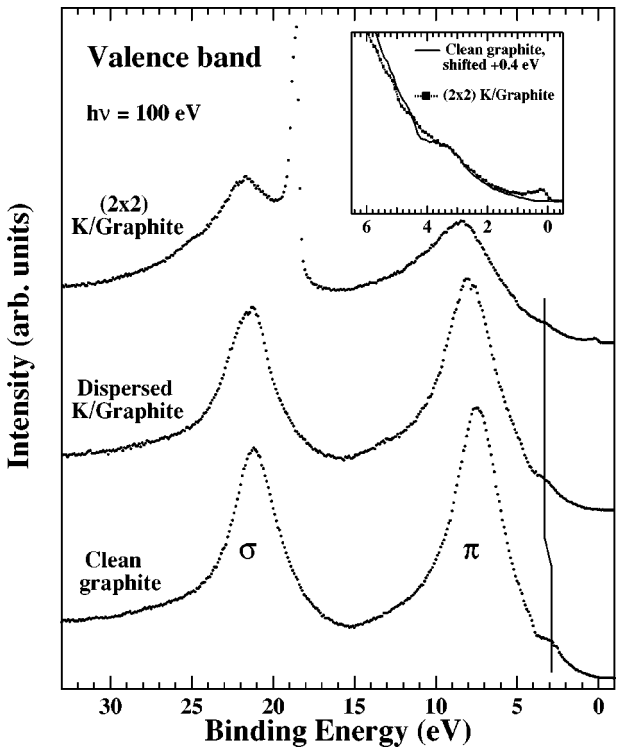

FIG. 1. Valence PES region for the indicated samples. The vertical line indicates the shift of the feature at 3 eV for clean graphite as a function of K phase, and the inset shows a detailed comparison of the data for the indicated samples.

As mentioned in the Introduction, the metallic character of the (2×2) phase manifests itself in EELS as a loss peak at 2.7 eV (K surface plasmon) and a broad feature at 0.5–1.2 eV (of more uncertain origin). A detailed comparison of the clean and (2×2) valence spectra in the regions of the band maxima leads us to conclude that the high-energy asymmetries are most likely due to these loss peaks within the overlayer, a combination of so-called extrinsic and intrinsic loss peaks associated with the graphite photoemission. The ''parent'' peaks are thus the graphite valence band itself and the K 3*p* peaks at 18.5 eV. Such loss features in the C 1*s* spectrum are discussed in Sec. III C.

Hence, the overall shape is very different compared to the clean graphite spectrum, and this makes it difficult to deduce any possible binding-energy shift between the clean and (2×2) situations. Nevertheless, examination of the spectra in the vicinity of the Fermi level reveals that there is a plateau-like feature with an onset at 3.3 eV, which, although weaker, remains after K deposition. The monotonic intensity increase, from E_F up to the beginning of the plateau, limits significant effects of extrinsic loss features to the high-energy side of the plateau, which becomes smeared out for the (2×2) phase. Therefore, a comparison was made between the clean and the (2×2) spectrum in the region from E_F to the ridge of the plateau (indicated in the inset of Fig. 1), and from this we deduce a shift of 0.4 ± 0.1 eV. This implies that the binding-energy shifts with respect to clean graphite for the valence bands in both the saturated dispersed and the (2×2) phase are the *same* to within an uncertainty

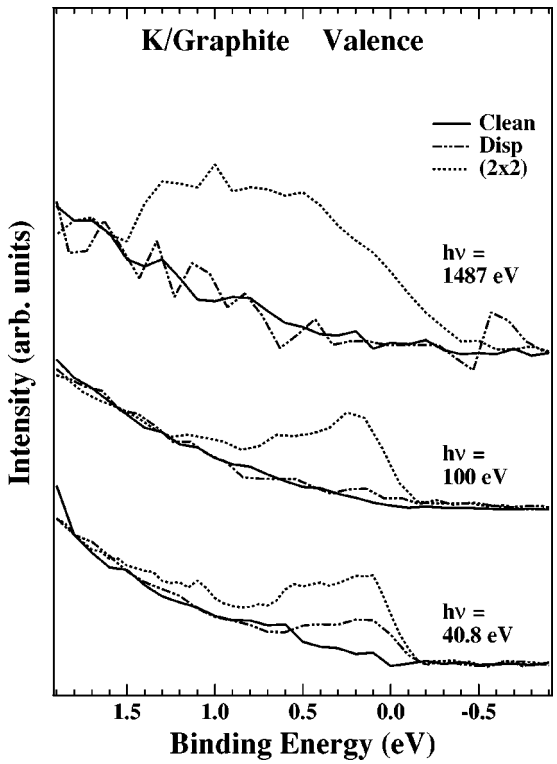

FIG. 2. Valence-band photoelectron spectra near E_F for the indicated samples, and at the indicated photon energies.

of 0.1 eV. This suggests a significant charge transfer from the (2×2) layer to the graphite substrate, which we will discuss in more detail in Sec. III C.

2. Near-Fermi-level region; 0–2 eV

The enhancement just below E_F for the (2×2) phase in Fig. 1 bears on the question of charge transfer, as mentioned in the Introduction. It is therefore interesting to further investigate to what extent the observations can be explained in terms of a rigid bandlike filling, or if they are due to a more complex potassium-induced modification of the band structure. The bands around the Fermi level for pure graphite have C $2p$ character. We can then describe the observed states at E_F for the adsorbate systems as predominantly K $4s$ and/or C $2p$ in character, and this is the question we will now address.

We utilize the fact that the C $2p$ and K $4s$ levels have different photon-energy-dependent cross sections, a fact which has been used previously in a study of GIC's,[24] and in the photoemission studies previously mentioned.[15] In particular, the theoretical[25] cross section at a photon energy of 1487 eV for the K $4s$ level is sufficiently high to allow it to be detected if present, whereas the cross section is nearly five times less for C $2p$ states. The cross section for the C $2p$ level increases gradually with lower photon energy, and becomes large enough in the uv region to allow changes near the Fermi level to be detected. With this in mind, we recorded the valence region near E_F at three different photon energies for clean graphite and the dispersed and (2×2) K phases.

The spectra are displayed in Fig. 2, in which each set contains data for a single photon energy and compares the different characteristic K coverages. The clean spectra are included as a background reference for the other data. The data with $h\nu=1487$ eV,100 eV, and 40.8 eV have total energy resolutions of 0.8 eV,0.3 eV, and 0.4 eV, respectively.

In the data taken at 1487 eV, the only spectrum which displays an enhancement at E_F is that for the (2×2) coverage. The cross-section argument thus leads us to conclude that the (2×2) phase involves states at E_F with significant K $4s$ character, whereas no K $4s$ states are seen for the dispersed phase. Nothing can be said about the C $2p$ character, since the cross section is too low. The data set at $h\nu=100$ eV merely magnifies parts of the spectra shown in Fig. 1, and again we find that only the (2×2) spectrum displays an enhancement at E_F. The width of the K-induced band in these higher-resolution data is around 1 eV. Finally, the data recorded at $h\nu=40.8$ eV show an enhancement at E_F for both the (2×2) and dispersed phases. Combined with the fact that the dispersed phase shows no E_F intensity at $h\nu=1487$ eV, we conclude that the K-induced states responsible for this feature must be of dominantly C $2p$ character for the latter phase. A remaining uncertainty after these measurements is the degree of C $2p$ character in the (2×2) K-induced Fermi level states, due to interference from the overlapping K $4s$–induced band(s).

To summarize, the *saturated* dispersed phase[26] displays an enhancement at the Fermi level which has mainly C $2p$ character, whereas the enhancement in the (2×2) phase has K $4s$ and possibly C $2p$ character. The evidence for the K $4s$ character for these states in the (2×2) phase is in direct contradiction to the previous photoemission studies.[14–16] Thus, our results confirm the picture of a charge transfer from K to graphite in the dispersed phase and the formation of a metallic K $4s$–derived band in the (2×2) phase.[9] We stress again that analysis of the near-E_F valence data does *not* exclude that charge is still donated from the potassium overlayer to the graphite in the (2×2) phase.

We also note that the dominating C $2p$ character in the 40.8 eV dispersed phase spectrum provides the possibility to directly estimate the band filling due to charge transfer for the *saturated* dispersed phase, within the rigid band model. For this purpose we use the calculated DOS shown in Fig. 3, and the data in Fig. 2. Based on trial and error the best agreement was achieved with a truncation of the calculated DOS at $E_F+0.6$ eV combined with a shift of 0.6 eV for alignment with the experimental spectrum, as shown in Fig. 4. It is useful to note that self-energy effects are found to increase the bandwidths of pure graphite by about 14%.[28] This implies a corrected shift in the present case of 0.5 eV.[29] Slightly smaller rigid band shifts are determined by direct comparisons between data for the clean and doped surfaces, as discussed in Secs. III A 1 and III C. In order to convert a binding-energy shift to charge transfer, we integrate the charge in the DOS corresponding to shifting E_F by that much (see Fig. 3). We then multiply by the number of C atoms per K atom, which for the saturated dispersed phase corresponds to a (7×7) unit cell as described above, multiplied by two atoms per clean-surface unit cell. Thus in the present case, a 0.5 eV shift implies a charge transfer of 98

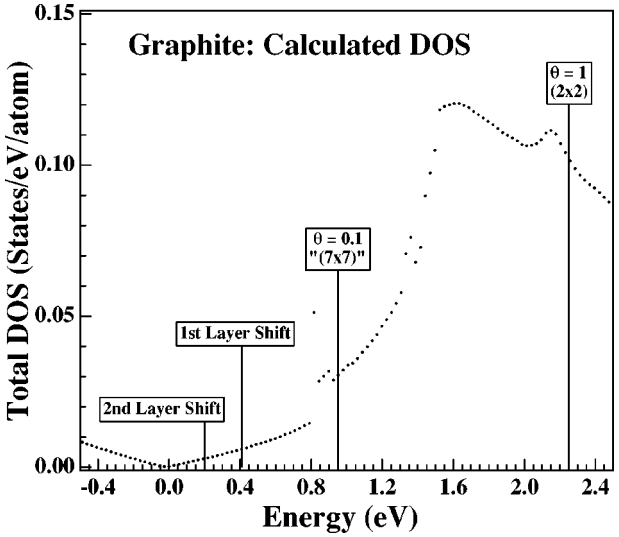

FIG. 3. Calculated DOS for clean graphite based on Ref. 27, used for charge transfer estimations. The ''1st'' and ''2nd layer shift'' correspond to the deduced shifts in Sec. III C 1 a, from which the charge transfers were calculated. On the other hand, the labels marked with $\Theta = 0.1$ and 1 ML correspond to the calculated rigid band shifts at these coverages under the assumption that each K atom donates exactly one electron.

$\times 0.0018 = 0.18e$ per K atom, which represents the upper limit of the values we extract from our data for the saturated dispersed phase; another estimate which confirms this result is based on the C 1*s* spectra and is presented in Sec. III C 1.

B. K 3*p*

Figure 5 shows the K 3*p* level for five different coverages. The coverages range from less than 1 ML (a dispersed and a mixed phase) through one 1 ML [the (2×2) phase]

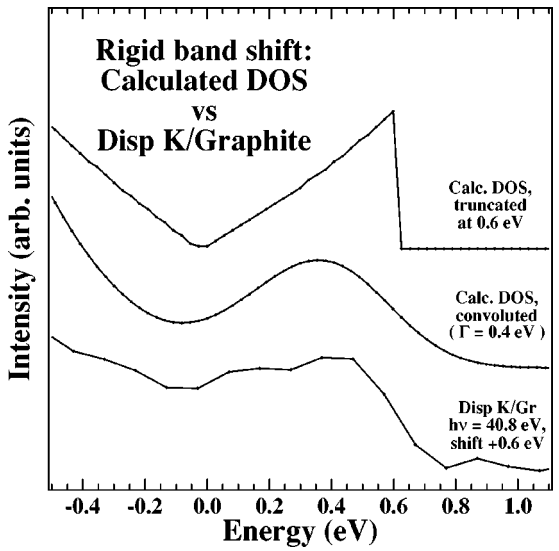

FIG. 4. Illustration of the procedure used to estimate the rigid band shift based on the $h\nu = 40.8$ eV spectrum for the *saturated* dispersed phase K/graphite (see Fig. 2) and calculated DOS for clean graphite (see Fig. 3). The calculated DOS was convoluted with a Gaussian line profile corresponding to the experimental resolution of 0.4 eV. See text for more details.

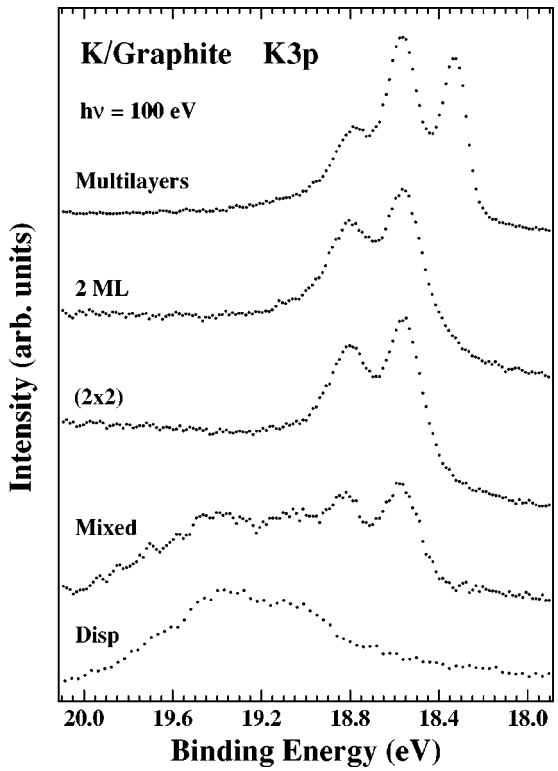

FIG. 5. K 3*p* PES at the specified coverages.

and above (2 ML and multilayers). The background due to the graphite σ bands has been estimated from the corresponding clean spectrum, and is subtracted in the two bottom spectra.

1. K 3p in the dispersed region

In the dispersed phase the K 3*p* spin-orbit doublet is quite broad and has a binding energy of roughly 19.4 eV ($K3p_{1/2}$) and 19.1 eV ($K3p_{3/2}$), respectively. Based on the idea that there could be a coverage-dependent screening of the K 3*p* emission due to dipole-dipole interactions or other K-K interactions via the charge donated to the substrate, we have attempted to detect an evolution of the K 3*p* spectrum as a function of coverage within the dispersed phase coverage range. However, even for the lowest coverages, where it is possible to see coverage-dependent shifts in the C 1*s* line (see Sec. III C 2), there is no evidence of a shifting K 3*p* line. This suggests that neither the so-called depolarization effect of neighboring image-potential-induced dipoles, nor a ''charge pool'' associated with each K adatom, has any role in the observed binding energy for coverages below the dispersed-to-(2×2) phase transformation. This is partially consistent with the estimate of Li *et al.*[10] of the charge transfer per K atom in the dispersed phase, in that within their model for the graphite charge carrier plasmon energy this charge transfer was practically constant over the entire coverage range.

The width of the dispersed phase K 3*p* spin-orbit doublet partners is about 400 meV, which is much broader than for the (2×2) phase. It is possible to model them as a broadened version of the narrower (2×2) lines. There are several possible sources for this increased broadening: (a) a distribu-

tion of neighbor interactions (dipole-dipole repulsion), suggested by the distribution of neighbor distances implicit in the width of the LEED peak for this phase;[9] (b) K-graphite vibrations; (c) a distribution of K-graphite interactions, i.e., different sites; and/or (d) lifetime broadening due to hybridization between the K $3p$ level and the graphite valence band.

Alternative (a) is possible to rule out as the dominant contribution. To see this, we consider the highest coverage under the onset of the phase transformation, for which the width of the LEED line indicates a nearest neighbor distribution of roughly 14 ± 2 Å or narrower. Using in our model the charge transfer of $0.7e$ suggested by EELS data combined with model calculations,[10] the dipole-dipole interactions vary from 25 to 80 meV, with a median of about 45 meV. If we take our own direct estimate of the charge transfer for this phase [See Sec. III C 1 a] of $0.15e$ per K atom, the broadening from this source is less than 20 meV. We assumed for these estimates a K-graphite distance of 2.75 Å in accord with the calculations of Ref. 30. Thus this appears to be a quite minor source of spectral broadening.

The role of vibrations (b) is difficult to estimate quantitatively. In order to get a general idea of the effect, one can assume for the ground state bonding purely via the image potential, and with a steep exponential barrier for distances closer to the surface than the ideal. For the ionized case, for which we assume a charge of one greater than the ground-state charge transfer, the origin of the potential is assumed to move closer to the surface by 0.3 Å, which is the change in ionic radius from K to Ca, the $Z+1$ element. The image potential is now steeper, so that the potential has a much larger slope at the ground-state origin point. Numerical estimates based on this crude picture suggest that such vertical vibrations could easily account for the observed broadening for reasonable values of the charge transfer.

We tentatively rule out (c), since the samples are prepared at 90 K where the K atoms have high mobility, and move to sit far apart.[9] It is therefore natural to assume that they adopt the optimum site, which according to theory[30] is the hollow site.[31] This was found to be favored by 80 meV over an on-top site, which was the only other possibility investigated there. Since this is large compared to the K-K interaction at all except the very smallest distances found for the dispersed phase, there is no apparent barrier to the optimization of the K-graphite interaction. The fact that the width of the K $3p$ line is, within experimental accuracy, of the same order of magnitude throughout the dispersed coverage range supports this idea, since there is no compensating increase in broadening from other sources.

Evidence for the importance of (d) for Cs adsorbed on metals has been reported recently, in which the low binding energy of the outermost core levels was suggested to lead to a significant role for the substrate electrons in the decay of the core hole.[32] The substrates in those cases were sp metals with relatively delocalized and isotropically distributed electrons in the valence band. For graphite, however, the bands in the relevant energy range have σ character, which implies that they will have minimal interaction with a level localized on adsorbed K atoms. Thus we tentatively rule out this source of broadening. We therefore conclude that K-K interactions and K-graphite hybridization contribute a minor fraction of the observed broadening in the dispersed phase, whereas K-graphite vibrations upon photoionization contribute the dominant fraction.

2. K 3p at higher coverages

a. Mixed phase. In the next spectrum shown in Fig. 5 (mixed phase), a new K $3p_{1/2,3/2}$ spin-orbit doublet is seen at 18.80 and 18.58 eV, respectively. The doublet associated with the dispersed phase is at the same binding energy as before. The new doublet is associated with K in the (2×2) phase, as is clearly evident from the 1 ML spectrum where the (2×2) phase is fully developed, and where no trace of the dispersed phase remains. The widths of the (2×2) peaks are greatly decreased in comparison to the dispersed phase. The cause of the observed shift is the more efficient metallic screening in the (2×2) phase. We note that the coexistence of the two phases is in accord with EELS findings.[9]

b. 2 Ml. Figure 5 displays also a spectrum for the 2 ML situation, for which almost no differences are observed: there are basically two peaks at the same energies as for 1 ML, although they are somewhat broader. The virtually identical binding energies of the two layers may seem surprising, since one layer is coordinated to graphite and the other has no bonds in the vacuum direction (which can be described[33] usefully as being coordinated to vacuum). In terms of nearest-neighbor distributions the two layers can be viewed as a surface layer and an interface layer. The results thus imply that the interface shift is very similar to the surface core-level shift. This is contrary to the normal situation for alkalis adsorbed on metal surfaces, as we discuss in more detail immediately below. Another observation for metallic interfaces is that the shifts to a rather good approximation are additive.[33] In such a situation one would expect for the monolayer a peak position which is shifted from the bulk peak position by the surface shift plus the interface shift. This is clearly not the case, which indicates that the K-graphite interaction is significantly altered as the second layer is deposited. That is, the binding-energy shift expected due to the change in the environment of the first layer due to the second layer is apparently compensated for by a change in the bonding of the first layer to the substrate.

c. Multilayer. In the multilayer case the surface (and interface) peaks at 18.80 and 18.58 eV are still seen, whereas a new component appears at 18.32 eV. This is due to the K $3p_{3/2}$ level in bulk K. The corresponding K $3p_{1/2}$ peak explains the increased intensity at 18.58 eV when compared to the 2 ML spectrum. Very similar spectra are obtained for multilayers of K deposited on metallic substrates.[34–37] In those cases, however, a third doublet is seen at lower binding energies due to potassium at the interface. The interface shift of the potassium core levels is thus very different for metal substrates and for graphite. For metal substrates the shift to lower binding energies can be explained in terms of repulsive contributions to the K-substrate bonding which are relaxed for a core ionized site. The fact that the graphite-induced shift is very similar to the surface core-level shift indicates that the metal/graphite bonding interaction changes very little due to the core ionization and/or that it is very

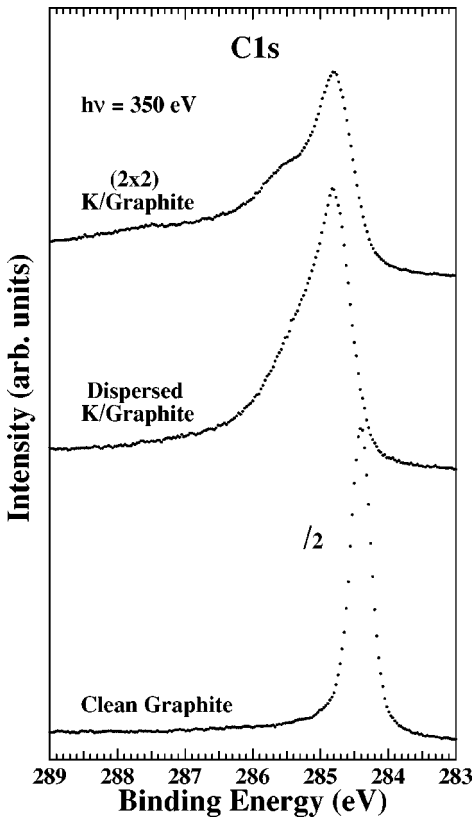

FIG. 6. C 1*s* spectra recorded for the indicated samples (normal emission).

weak, and therefore has a negligible effect on the K 3*p* binding energy.

C. C 1*s*

In this section, the shift and line profile of the C 1*s* level will be discussed extensively. As a prelude, Fig. 6 displays the C 1*s* line for three situations, namely clean graphite, the saturated dispersed phase (0.1 ML), and the (2×2) phase (1 ML). The spectra are recorded with $h\nu=350$ eV and are normalized to give equal area in the displayed region, except for the clean graphite spectrum which is divided by an additional factor of 2. The chosen normalization is arbitrary and does not reflect any physical property.

The C 1*s* line for clean graphite has a binding energy of 284.4 eV and a full width at half maximum (FWHM) of 0.36 eV. The line shape for the saturated dispersed phase is much broader and has shifted 0.4 eV towards higher binding energy to 284.8 eV. The spectrum of the (2×2) phase shows the same peak shift of 0.4 eV, whereas the spectral shape is even broader. A shoulder at 285.5 eV and a broad feature centered at around 287.5 eV are clearly present.

In the following sections we will consider the shift and line profile of the C 1*s* level using different approaches, in an attempt to illuminate the origin of these features. This includes investigations of the consequences of applying the rigid band model. We consider the dispersed and (2×2) phases separately.

1. C 1s in the dispersed phase

As was seen in Fig. 6, the line profile of the C 1*s* level changes considerably when going from clean graphite to the dispersed phase. At the same time, the peak shifts 0.4 eV towards higher binding energy. This section deals with the likely sources for the C 1*s* line shape and position. We assume that there are three basic contributions to consider: (a) contributions from different graphite layers; (b) different C sites both within one layer, and/or between different layers; and (c) electron-hole pair excitations or other satellite processes.

a. Binding energy shift(s) and layer-resolved spectra. In order to resolve the contributions from different layers, it is necessary to know the mean free path (MFP) of the photoelectrons measured. As is well known, using the MFP, the intensity from a certain layer can be estimated by an exponential function describing the attenuation. Furthermore, by angle-resolved measurements it is possible to vary the escape depth of the photoelectrons, and thus the probe depth. This is expressed in Eq. (1):

$$I_n = I_0 \exp(-nx/(\lambda \sin \phi)), \tag{1}$$

where I_n is the intensity from the nth layer, I_0 is the total intensity, x is the interlayer distance, ϕ is the emission angle, and λ is the MFP. We make the implicit assumption that the surface is atomically smooth.

The C 1*s* spectra presented so far were recorded with $h\nu=350$ eV, but the MFP for electrons at the corresponding kinetic energies (around 65 eV) is very low, and therefore could not be used for this purpose. However, the MFP measured for a kinetic energy of 1169 eV was found[38] to be 18 Å. With a photon energy of 1487 eV, the kinetic energy of C 1*s* electrons is around 1204 eV, and we therefore assume that the MFP is 18 Å.

With this in mind, we recorded angle-resolved spectra for the saturated dispersed phase shown in Fig. 7. All spectra are normalized to equal areas in the shown energy window, 283–289 eV, which was chosen to include most of the line without entering the region where a graphite π-plasmon loss peak appears at around 291 eV. It is seen that for decreasing emission angles, i.e., increasing surface sensitivity, the C 1*s* line shape becomes broader and shifts towards higher binding energy. The resolution of these spectra is poorer than in the $h\nu=350$ eV spectra, and decreases with decreasing angle. In order to monitor the angle-dependent resolution, we also recorded angle-resolved spectra for clean graphite (not shown). The clean spectra were also used in the curve fits described below.

If we assume that the MFP is the same for the dispersed phase as for clean graphite, Eq. (1) makes it possible to calculate the contribution of each layer to the total intensity in each of the angle-resolved spectra. Based on this idea we carried out a curve fit where two approaches were used.

In the first approach, the 5° spectrum was used as a template for the first layer, assuming that it contained intensity from the first layer only [rather than 90% first layer as expected using Eq. (1) with a MFP of 18 Å]. The underlying (bulk) layers were then modeled with clean spectra as templates. The intensity for all template spectra was scaled according to Eq. (1). Briefly, the curve fits indicated (via the shift for each layer) that there is a charge transfer to the first *and second* layers, whereas our modeling of the data suggests that charge transfer to the third layer is negligible com-

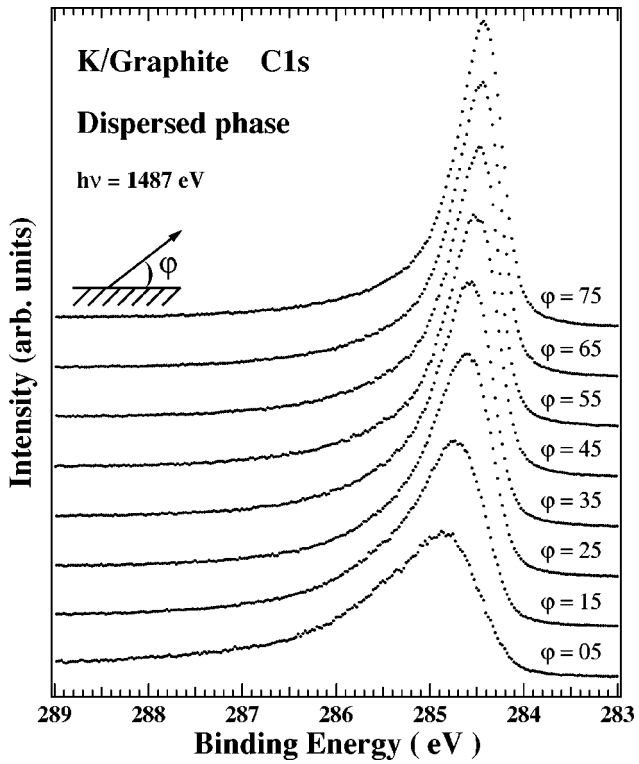

FIG. 7. Angle-resolved C 1*s* spectra for the saturated dispersed phase at the indicated photon energy. The surface sensitivity increases with decreasing emission angle, indicating that only the topmost layers are influenced by the potassium.

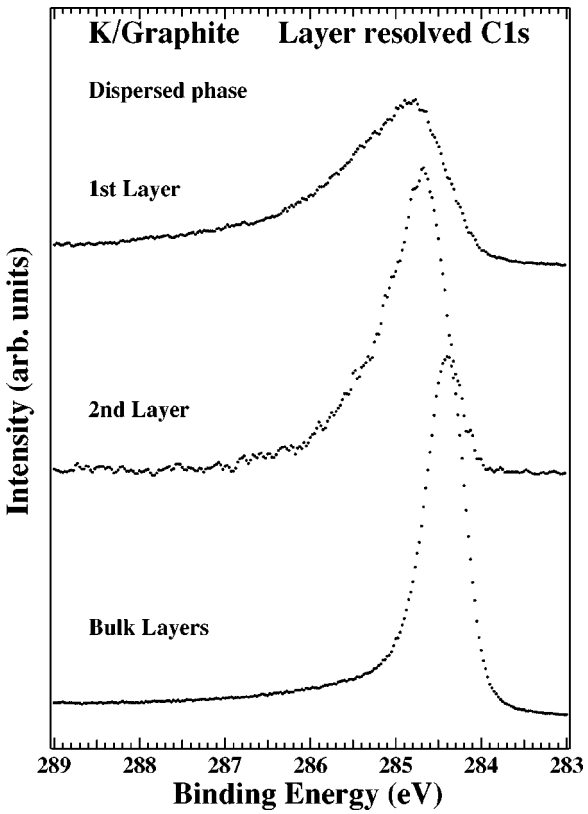

FIG. 8. Layer-resolved C 1*s* spectra for the dispersed phase, obtained by a subtraction procedure described in the text from the data in Fig. 7.

pared to the second layer. However, precisely because of the charge transfer to the second layer, it is not appropriate to use a clean spectrum as a template, and for this reason a second curve fit was carried out.

The next level of complexity therefore involved determining a line shape for the second layer spectrum. In order to accomplish this with a minimum of model dependence, we carried out a series of subtractions with different combinations of the 5° and 15° dispersed phase spectra and the 15° clean spectrum, where the clean spectrum was used as a template for the unaffected bulk layers (third layer and beyond).

Equation (1) indicates that the 5° dispersed spectrum contains intensity from the first (90%) and second (10%) layers only, whereas the 15° spectrum contains about 50% from the first, 25% from the second, and 25% from the rest of the layers. By proper renormalization of the spectra (within the given energy range of 283–289 eV), the intensity was set such that the relative amount from the first layer was the *same* in both the 5° and the 15° spectra, which allowed a subtraction that removed this intensity completely. The subtracted spectrum then contained intensity only from the second and deeper layers. The intensity of the deeper layers was then removed by a new subtraction involving the clean 15° spectrum (properly normalized), which gave a subtracted spectrum containing only intensity from the second layer. Finally, obtaining the first layer merely required that the obtained second layer spectrum was subtracted from the 5° spectrum (after a new normalization).

It is clear that the relative shifts among the spectra are important parameters in these manipulations, which makes proper energy calibration essential. We estimate the calibration error to be ± 0.05 eV, and therefore allowed variations within this range. The best results from this procedure are presented in Fig. 8. The first layer has essentially the same shape as the 5° dispersed spectrum, and has a binding energy of 284.8 eV. The second layer has a line which is broader than that of the 15° clean spectrum but narrower than the first layer spectrum, at a binding energy of 284.6 eV.

Although both the binding energy and detailed line shape of the second layer should be treated with some skepticism, there is no doubt that, within the model used to derive Eq. (1), the potassium overlayer also influences the *second* layer. This is in line with the finite interlayer interaction obtained in an *ab initio* density-functional calculation[39,40] on pure graphite, where it was found that the interplanar bonding consists of both van der Waals forces and a chemical interaction of almost equal strength. The latter is described as an electronic delocalization which gives rise to a small enhancement in the charge density between the layers, i.e., in the *z* direction (where *x* and *y* are the in-plane coordinates).

We can now estimate what the rigid band model yields in terms of the amount of transferred charge for the saturated dispersed phase. If we assume that screening effects in the photoemission process can be excluded (as we motivate in detail in the following section), we can use Figs. 8 and 3 to derive the charge transfer per C atom using the C 1*s* shift of the first and second layer relative to the clean (or bulk) C 1*s* binding energy of 284.4 eV. This yields 0.0012e/C atom for the first layer (shift of 0.4 eV) and 0.0003e/C atom for the second layer (shift of 0.2 eV), respectively. The DOS shift

derived above in Secs. III A 1 and III A 2 based on two separate analyses of the valence-band data is quite similar to the first layer C 1*s* shift derived here, giving us confidence in the numbers we obtain.

The charge transfer per K atom, which corresponds to the charge accepted by the graphite as derived here for the saturated dispersed [i.e., (7×7)] phase, is approximately $98\times(0.0012e+0.0003e)=0.15e$. Interestingly, the C 1*s* line does not shift over a wide K coverage range (except for very small K coverages, see Sec. III C 2), implying that the total charge transfer is constant over most of the coverage range from 0–0.1 ML. This suggests that the charge transfer per K atom goes down as a function of coverage, in qualitative agreement with the calculated trend,[41] but in disagreement with the muffin-tin occupation of a more recent calculation.[42] It also disagrees with EELS results[10] where a constant charge transfer of $0.7e$ was derived combining the dispersed phase charge-carrier plasmon energy with model calculations. Finally, we point out that the absolute value of charge transfer for the highest density dispersed phase found here using a rigid band model analysis is well under calculated[30,42] values near $0.3e$, though these can be difficult to interpret.[42]

b. Line shape. Having established that charge is donated to two graphite layers in the dispersed phase, and that both layer-resolved C 1*s* spectra are asymmetric, we next address the question of the origin of this strong asymmetry. We will again use spectra recorded with $h\nu=350$ eV because the resolution is higher for these spectra than the XPS spectra shown in the preceding section. As mentioned, the MFP is unknown at kinetic energies of around 65 eV, but it is expected that it is low in accordance with the universal curve of MFP's for all elements. It is impossible to achieve a completely consistent description of the data without a direct measurement of the mean free path at these relatively low kinetic energies. There are two salient points to note: (i) The first-layer spectrum derived from the angle-resolved XPS data is quite similar to the 350 eV spectrum, as is the grazing emission XPS spectrum which must be dominated by the first layer; (ii) if our model were perfect at XPS kinetic energies, the lack of a second-layer component in the 350 eV data suggests that there is a very low mean free path (<3 Å) for the dispersed phase case. We find that there is only a weak sensitivity to the mean free path used for the XPS analysis, varying the value used by $\pm30\%$. However, since the low implied value for a kinetic energy of 65 eV is difficult to justify without experimental proof, a conclusive test of the accuracy of our model is impossible. Nevertheless, the basic thesis remains that charge is transferred to the second layer.

The asymmetry we observe can either be due to different carbon sites and/or electron-hole pair excitations. It is tempting to assume that many sites are involved; this is common for adsorbates or complex compounds. On the other hand, in the dispersed phase there are no obvious site distribution effects seen using other techniques (see, e.g., Ref. 9 and Fig. 1). To model or resolve any postulated site effects via curve fitting is therefore difficult, as there are too many free parameters (e.g., the number of components, line shape, relative intensity, etc.).

We suggest instead that the dominant contribution comes from electron-hole pair (EHP) excitations, and that the width

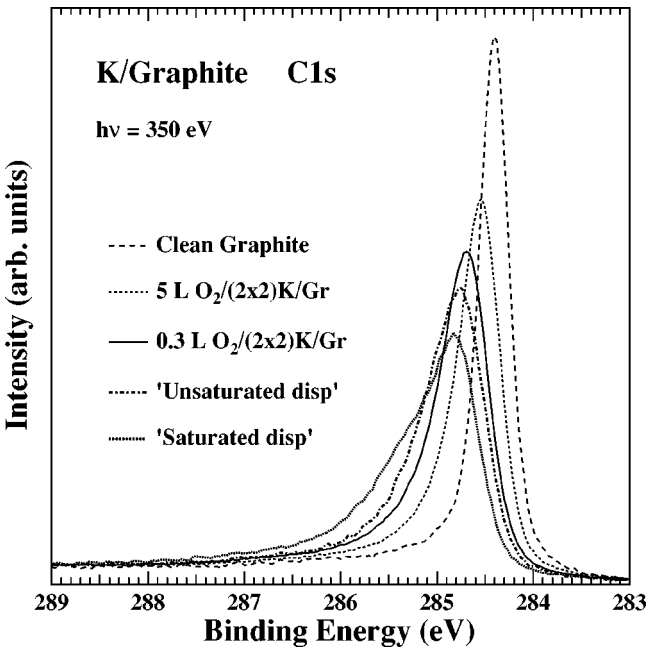

FIG. 9. C 1*s* spectra for samples corresponding to different charge transfers. The linewidth is seen to be correlated to the binding energy.

of the asymmetry is set primarily by the DOS. In support of this idea, Fig. 9 displays C 1*s* spectra for five samples chosen for the degree of charge transfer to the substrate: clean graphite, 5 and 0.3 *L* O_2 on a prepared (2×2) phase; an ''unsaturated'' (not fully developed) dispersed phase, and a saturated dispersed phase. The coadsorption systems with O_2 on (2×2) K/graphite are taken from Ref. 43, where the two different doses result in the formation of different K-O complexes which destroy the (2×2) overlayer, and, additionally, withdraw some of the charge from the graphite. In the 5 *L* O_2 case, there is little charge left. The spectra are arbitrarily normalized to equal areas in the energy window shown, and the emission is dominated by the contributions of the uppermost layers. This figure shows that, as the shift from the clean C 1*s* peak position increases, so does the width. This trend is qualitatively consistent with the rigid band model as well. In photoemission spectroscopy on core levels of metals, it is accepted that the typical asymmetry towards higher binding energy is due to electron-hole pair excitations. The asymmetry will thus depend on the shape and magnitude of the DOS near E_F. This applies also for graphite, and it is clear from the rigid band model and the particular band structure of graphite that when the empty DOS gradually becomes more filled, the asymmetry of the C 1*s* line shape will increase due to the increased phase space[44] for low-energy electron-hole pairs. Thus we find empirically that the C 1*s* XPS asymmetry can be used as an independent measure of the charge donated to the graphite. We note that the C 1*s* line shape and binding-energy shift for the second graphite layer extracted via angle-resolved XPS is fully consistent with these arguments.

The shoulder at about 285.4 eV in the dispersed phase C 1*s* XPS line suggests an additional aspect to the shakeup, i.e., the presence of a discrete or quasidiscrete excitation. Continuing the discussion from the preceding paragraph, we

note that shakeup intensity in core-level photoemission is dominated by transitions from and to strongly relaxed orbitals.[45] As pointed out long ago from a more general standpoint,[46] this means that the large peak found in C 1*s* x-ray absorption of graphite just above the edge, which corresponds to strongly relaxed states described elsewhere as excitonic,[47–49] should play a dominant role for shakeup as the Fermi level approaches this feature, which lies at $E_F + 0.9$ eV for clean graphite.[48,49] C 1*s* absorption for alkali-intercalated graphite[50,51] as a function of intercalation stage shows that a rigid band picture positioning of the 1*s* exciton is qualitatively correct. In addition, the C 1*s* XPS line shape for dispersed K/graphite is difficult to explain as a Doniach-Sunjic profile, with too much intensity located at around 0.5 eV to higher binding energy than the peak (see previous analyses of the clean graphite case, Refs. 46 and 52).

With these observations in mind, it seems most reasonable to infer that the graphite 1*s* exciton is responsible for the change in the C 1*s* photoemission line shape with charge transfer, since as a final state it is moving closer to the main line. The greater occupied DOS at E_F in the ground state with greater doping would also contribute positively to this effect. The C 1*s* binding-energy shift of 0.4 eV for the dispersed phase places E_F at about 0.5 eV below the exciton in the rigid band model (assuming no net extra screening), as already noted, which is also quite suggestive. Effects of screening from other graphite layers are unlikely to be important, since the screening of a 1*s* hole (or N impurity) is already quite complete for an isolated and undoped graphene sheet,[53,49] just as it is for smaller aromatic carbon systems.[54,55] This suggests that the addition of charge to the unoccupied bands will not significantly change this screening. The latter assertion is supported by the rigid-band-like shifts of the σ-like valence levels and C 1*s* level of C_{60} adsorbed on metal surfaces.[56] Since calculation of the shakeup distribution for this system is beyond present theoretical capabilities, we can go no further with this analysis.

2. C 1s in the (2×2) phase

This section focuses on the characteristic line shape of the C 1*s* level in the (2×2) phase. In Fig. 6, it was seen that a shoulder at around 1 eV from the maximum peak position and a broad feature at around 2.7 eV are the main differences when going from the dispersed to the (2×2) phase.

Figure 10 displays C 1*s* spectra, recorded at $h\nu = 350$ eV and arbitrarily normalized to equal areas in the energy window shown. The coverages range from an unsaturated dispersed phase to a saturated dispersed phase, a mixed phase, and finally a (2×2) phase. Focusing on the shoulder at 285.5 eV, it is clear that it is not present in the unsaturated dispersed spectrum, but then grows as the coverage increases until it is quite distinct in the (2×2) phase. If we then turn to the feature at 287.5 eV, a similar behavior is seen where the feature is most pronounced in the (2×2) phase. Finally, we note that the main peak position stays constant at 284.8 eV during the dispersed-to-(2×2) phase transformation.

Before we go into detail, two remarks are required. First, the unsaturated dispersed phase spectrum presented in this section corresponds to a very small coverage, far below what we refer to as the saturated phase (0.1 ML). In fact, the

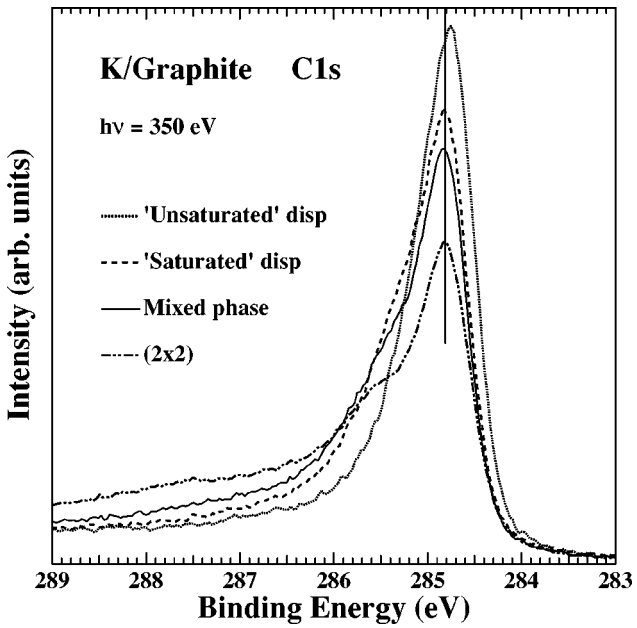

FIG. 10. C 1*s* spectra for the dispersed-to-(2×2) phase transition. The main line position (284.8 eV) remains constant during the transformation, whereas the shoulder at 285.5 eV and broad structure at 287.5 eV increase with coverage.

binding-energy shift for the C 1*s* almost immediately goes to 0.4 eV and then stays there as a function of coverage within the dispersed phase. Second, we will assume that the spectra are surface sensitive, arguing in the same way as for the spectra presented in the preceding section. In fact, the same line shape and binding energies for the (2×2) phase were obtained in surface-sensitive XP spectra ($h\nu = 1487$ eV, not shown). Furthermore, an angle-resolved series (not shown) of C 1*s* spectra for the (2×2) phase was recorded, which displayed a similar behavior as compared to the series for the dispersed phase shown in Fig. 7. We thus believe that the spectra presented in this section are dominated by emission from the first graphite layer only.

We now attempt to understand the extra features that appear in the (2×2) spectra. One possibility would be to assume that the main peak at 284.8 eV is associated with one carbon site, and the smaller peak at 285.5 eV is a component associated with a different carbon site. This is quite plausible in principle when considering the unit cell for the (2×2) phase, shown in Fig. 11. In terms of distances to the K atoms (large dots), two types of carbons exist: nearest-neighbor (squares) and next-nearest-neighbor (small dots) C atoms, with a ratio of 3:1, equivalent to the required intensity ratio for a two-component decomposition of the (2×2) C 1*s* spectrum. In addition, the 287.5 eV feature has to be in-

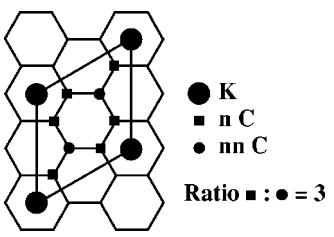

FIG. 11. Unit cell for (2×2) K/graphite.

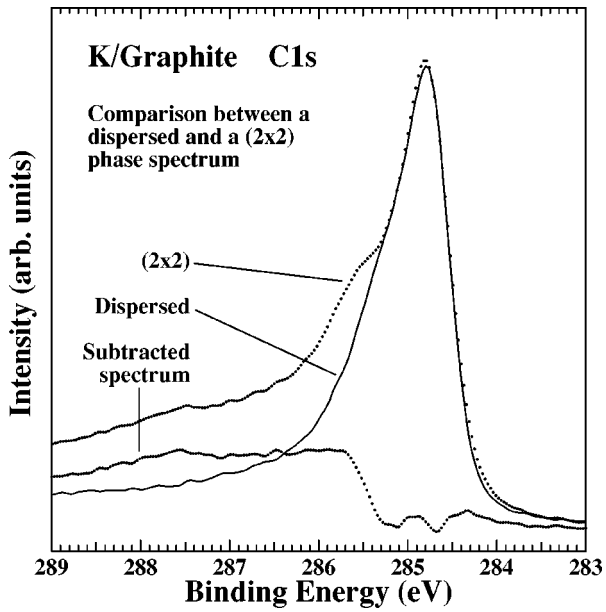

FIG. 12. Comparison between (2×2) and dispersed phase C 1*s* spectra. The difference spectrum suggests an interpretation of the (2×2) spectrum in terms of a dispersed spectrum with additional loss features associated with the (2×2) metallic overlayer.

cluded in the modeling, adding up to a three-component model. Therefore, we tried different curve fits to reveal these components, but despite using different combinations of, e.g., asymmetric Voigt profiles and/or templates based on a dispersed phase spectrum, unsatisfactory results were always obtained. In particular, in all the fits we obtained a main-to-shoulder peak ratio on the order of 5:1 rather than of 3:1, arguing against a site-dependent model.[57]

These results lead us to an alternative model for the (2×2) C 1*s* spectrum. The close similarity of the main component to the dispersed phase spectrum suggests an explanation in terms of satellites. Figure 12 displays a subtraction of the dispersed phase spectrum from the (2×2) spectrum, where the former is aligned and scaled as carefully as possible to the latter. The resulting subtracted curve is a broad distribution starting at around 285.5 eV. We suggest that it can be explained as solely due to a combination of extrinsic and intrinsic (shakeup) loss processes associated with the presence of the metallic (2×2) K overlayer. This is consistent with EELS data, for which the (2×2) phase is characterized by a broad feature between 0.5 and 1.2 eV, together with the 2.7 eV K surface plasmon.[9]

That the shift and shape are the same for the (2×2) as in the dispersed phase strongly implies that, in terms of the graphite first-layer charge state, there is *no significant difference* when transforming the dispersed to the (2×2) phase. This conclusion contradicts previous interpretations of EELS data for these systems, for which the disappearance of the charge-carrier plasmon at 0.32 eV associated with the dispersed phase was suggested to be due to withdrawal of charge in the dispersed-to-(2×2) phase transformation.[9] Instead, we propose a combination of two possibilities: (a) the substrate electrons do not respond to the potential of the EELS probe electron due to screening by the metallic overlayer, and/or (b) the substrate charge-carrier plasmon is strongly coupled to the electron-hole pair continuum of the overlayer, and thus has a much shorter lifetime. Alternative (a) is strongly supported by, e.g., EELS data for a Na monolayer on Al(111),[58] for which at least 80% of the Al surface plasmon intensity is quenched. The agreement of the shifts for the C 1*s* lines and those determined in the valence-band data suggests that the screening effects in core-level PES are similar and/or low for both cases, which may be a consequence of the small amount of charge donated per C atom. Thus we ascribe the discrepancy with EELS estimates of the charge transfer to screening effects in EELS.

Another ramification of a model in terms of loss processes concerns the GIC's. In several cases where the C 1*s* line has been studied,[16–20] shoulders similar to the 285.5 eV shoulder in our spectra appear in some of the published C 1*s* spectra, especially for stage-1 compounds (alternating alkali and graphite layers). The origin of the shoulder is often explained in terms of different C sites, but models based on this idea seem to have problems reproducing the line shape, as well as the intensity ratios suggested by structural considerations. In some cases such a shoulder is explained as being due to sample deterioration. Although the electronic structure of GIC's is somewhat different from the present systems, our results offer two alternative explanations that should be considered: First, since the samples used for XPS and UPS studies of GIC's of necessity are more difficult to characterize, so that, e.g., it is not always clear what surface composition is exposed in the cleaving process typically employed, it is tempting to speculate that a (2×2)-like alkali layer, in those cases on the surface of intercalated graphite, could lead to the observed phenomena; second, since the intercalate layers have metallic character, there should be a possibility for loss processes similar to the ones we suggest for the (2×2) alkali overlayer.

Finally, by using the rigid band model again, we conclude this section with an estimate of the charge transfer from each K atom to the graphite, for the (2×2) phase. The C 1*s* shift is the same as for the saturated dispersed phase, and assuming that the second layer is influenced also for the (2×2) phase this yields $8\times(0.0012e+0.0003e)=0.012e$.

IV. CONCLUSIONS

(a) The C 1*s* main line binding-energy shift (0.4 eV) and line shape for the dispersed and the (2×2) phase are the same, as are the valence level binding-energy shifts (also 0.4 eV) relative to clean graphite. It is only for *very* small potassium coverages that we observe a C 1*s* binding-energy shift of less than 0.4 eV. This implies that the *total* donated charge from the potassium to the graphite is almost constant for all coverages.

(b) Charge transfer is quite small over the entire coverage range: the fact that the shifts of the C 1*s* line and valence band are the same indicates a quite minor role for screening in determining the binding energy shift of the C 1*s* line. Thus, based on the C 1*s* binding-energy shift in combination with calculated DOS for clean graphite, we obtain a transferred charge per K atom to be $0.15e$ (Sec. III C 1) and $0.012e$ (Sec. III C 2) for the saturated dispersed phase and the (2×2) phase, respectively.

(c) For the saturated dispersed phase, we find that charge is also donated to the *second* graphite layer, and we assume

that this holds also for the (2×2) phase. The numbers given above for the charge transfer per K atom are based on these results.

(d) Further strong evidence (Sec. III A 2) for the magnitude of the charge transfer in the saturated dispersed phase is given in the 40.8 eV spectrum, where the enhancement at E_F is associated with the π band only; no overlapping K 4*s* is detected. Based on a comparison of the shapes of the theoretical and experimental valence-region data, the width of the upper π band is around 0.5 eV. Within the rigid band model, this band corresponds to the filled region of the previously unoccupied DOS above the Fermi level, and the theoretical value of 0.5 eV fits quite well with the observed shift of 0.4 eV for the C 1*s* line and the valence band. This puts the range of possible charge transfer based on the present work at $0.15e-0.18e$ per K atom for the saturated dispersed phase.

(e) The C 1*s* line shape in the dispersed phase is attributed to intrinsic electron-hole-pair excitations. The shift and the width follow each other in a consistent manner (more charge transfer results in a larger shift plus a broader line). For the dispersed phase, the shifting and broadening process saturates at a very low charge transfer. We speculate that the unique line profile for the dispersed phase arises due to the semimetal character of graphite and the strong core hole effects[47,49] on the DOS.

(f) The C 1*s* line shape in the (2×2) phase can be understood as being identical to that of the dispersed phase spectrum, modified by extrinsic losses associated with the metallic overlayer.

(g) The C 1*s* data in intercalation compounds generally involve larger shifts (around 1 eV) and are broader; this is consistent with the reasoning above, since a greater degree of charge transfer per K and per C atom is expected. Satellites similar to those we observe are often observed for these systems, whose origin has been difficult to establish. Our results suggest that this may simply be a consequence of the surface morphology, or due to loss processes within the metallic intercalation layer.

(h) The present results on the charge transfer for coverages less than 0.1 ML are in disagreement with other studies, in that the numbers we obtain are lower. We have no satisfactory explanation for this, but note that our results are self-consistent.

ACKNOWLEDGMENTS

The technical support provided by J.-O. Forsell and L. Bolkegård, Uppsala, and help from the staff at MAX-Lab are gratefully acknowledged. We received helpful input from E. L. Shirley and O. Gunnarsson. Special thanks go to R. Ahuja for providing the band-structure calculations on pure graphite, and to A. W. Moore for providing the graphite samples. This work was supported by the Human Capital and Mobility Program of the European Community, HCM network Contract No. CHRX-CT94-0580; NFR, the Swedish Natural Science Research Foundation; the Consortium on Clusters and Ultrafine Particles, which is funded by NFR and NUTEK, the Swedish Board for Industrial and Technical Development; and the Belgian National Fund for Scientific Research.

[1] *Physics and Chemistry of Alkali Metal Adsorption, Material Science Monographs Vol. 57*, edited by H.P. Bonzel, A.M. Bradshaw, and G. Ertl (Elsevier, New York, 1989).
[2] G.K. Wertheim, D.M. Riffe, and P.H. Citrin, Phys. Rev. B **49**, 4834 (1994).
[3] *Graphite Intercalation Compounds I*, Springer Series in Material Sciences Vol. 14, edited by H. Zabel and S.A. Solin (Springer-Verlag, Heidelberg, 1990).
[4] M.S. Dresselhaus and G. Dresselhaus, Adv. Phys. **30**, 139 (1981).
[5] M.S. Dresselhaus, *Intercalation in Layered Materials* (Plenum, New York, 1987).
[6] M.S. Dresselhaus, G. Dresselhaus, and J.E. Fischer, Phys. Rev. B **15**, 3180 (1977).
[7] *Solid State Physics*, edited by H. Ehrenreich and F. Spaepen (Academic, New York, 1994), Vol. 48.
[8] K.M. Hock and R.E. Palmer, Surf. Sci. **284**, 349 (1993).
[9] Z.Y. Li, K.M. Hock, and R.E. Palmer, Phys. Rev. Lett. **67**, 1562 (1991).
[10] Z.Y. Li, K.M. Hock, R.E. Palmer, and J.F. Annett, J. Phys.: Condens. Matter **3**, S103 (1991).
[11] J.C. Barnard, K.M. Hock, and R.E. Palmer, Surf. Sci. **287/288**, 178 (1993).
[12] N.J. Wu and A. Ignatiev, J. Vac. Sci. Technol. **20**, 896 (1982).
[13] J.B. Swan, Phys. Rev. **135**, A1467 (1964).
[14] M.T. Johnson, H.I. Starnberg, and H.P. Hughes, Solid State Commun. **57**, 545 (1985).
[15] M.T. Johnson, H.I. Starnberg, and H.P. Hughes, Surf. Sci. **178**, 290 (1986).
[16] A.R. Law, M.T. Johnson, and H.P. Hughes, Surf. Sci. **152/153**, 284 (1985).
[17] B.R. Weinberger, J. Kaufer, A.J. Heeger, J.E. Fischer, M. Moran, and N.A.W. Holzwarth, Phys. Rev. Lett. **41**, 1417 (1978).
[18] M.F. Lin and K.W.-K. Shung, Phys. Rev. B **46**, 12 656 (1992).
[19] S.B. DiCenzo, G.K. Wertheim, S. Basu, and J.E. Fischer, Phys. Rev. B **24**, 2270 (1981).
[20] R. Schlögl, V. Geiser, P. Oelhafen, and H.-J. Güntherodt, Phys. Rev. B **35**, 6414 (1987).
[21] J.N. Andersen, O. Björneholm, A. Sandell, R. Nyholm, J.-O. Forsell, L. Thånell, A. Nilsson, and N. Mårtensson, Synchrotron Radiat News **4**, No. 4,15 (1991).
[22] A. Nilsson and N. Mårtensson, Phys. Rev. B **40**, 10 249 (1989).
[23] R.E. Palmer, P.V. Head, and R.F. Willis, Rev. Sci. Instrum. **58**, 1118 (1987).
[24] M.E. Preil and J.E. Fischer, Phys. Rev. Lett. **52**, 1141 (1984).
[25] J.H. Scofield, J. Electron Spectrosc. Relat. Phenom. **8**, 129 (1976).
[26] We emphasize that all charge-transfer estimates for the dispersed phase refer to the *saturated* coverage, above which (2×2) islands begin to form. For lower coverages we see almost the same shift in the C 1*s* line (see, e.g., Fig. 9), though slightly lower (see also the discussion in Sec. III B 1). We found it difficult to trace the development of the C 1*s* binding energy as a function of coverage due to the very low coverages involved and problems with coverage calibration.
[27] R. Ahuja, S. Auluck, J. Trygg, J.M. Wills, O. Eriksson, and B.

Johansson, Phys. Rev. B **51**, 4813 (1995).
[28] S.G. Louie, in *Computational Materials Science*, edited by C. Y. Fong (World Scientific, Singapore, 1997).
[29] We ignore the effects of K doping, which are unknown. However, doping of another low-dimensional aromatic solid, C_{60}, leads to contributions to the screening which decrease the bandwidths from what is found for the undoped case based on the formation of a plasmon at 0.5 eV[O. Gunnarsson, J. Phys.: Condens. Matter **9**, 5635 (1997)]. Since the plasmon which is affected by doping graphite is much lower in energy than that induced in C_{60}, we infer that any effects of doping in the present case should be insignificant.
[30] F. Ancilotto and F. Toigo, Phys. Rev. B **47**, 13 713 (1993).
[31] A weakness of this calculation is that the density of atoms chosen is not achievable for ordered overlayers, corresponding to a mixed phase.
[32] E. Lundgren, R. Nyholm, and J.N. Andersen, MAX Lab Activity Report 1995, p. 110 (unpublished).
[33] A. Nilsson, B. Eriksson, N. Mårtensson, J.N. Andersen, and J. Onsgaard, Phys. Rev. B **38**, 10 357 (1988).
[34] A.J. Maxwell, P.A. Brühwiler, S. Andersson, N. Mårtensson, and P. Rudolf, Chem. Phys. Lett. **247**, 257 (1995).
[35] T.K. Sham, G.-Q. Xu, J. Hrbek, and M.-L. Shek, Surf. Sci. **210**, L193 (1989).
[36] G.K. Wertheim, D.M. Riffe, N.V. Smith, and P.H. Citrin, Phys. Rev. B **46**, 1955 (1992).
[37] D.M. Riffe, G.K. Wertheim, and P.H. Citrin, Phys. Rev. Lett. **64**, 571 (1990).
[38] R.G. Steinhardt, J. Hudis, and M.L. Perlman, Phys. Rev. B **5**, 1016 (1972).
[39] J.-C. Charlier, X. Gonze, and J.-P. Michenaud, Europhys. Lett. **28**, 403 (1994).
[40] M.C. Schabel and J.L. Martins, Phys. Rev. B **46**, 7185 (1992).
[41] H. Ishida and R.E. Palmer, Phys. Rev. B **46**, 15 484 (1992).
[42] O. Hjortstam, J. M. Wills, B. Johansson, and O. Eriksson, Phys. Rev. B **58**, 13 (1998).
[43] C. Puglia, P. Bennich, J. Hasselström, P.A. Brühwiler, A. Nilsson, A.J. Maxwell, N. Mårtensson, and P. Rudolf, Surf. Sci. **383**, 149 (1997).
[44] E.T. Jensen, R.E. Palmer, W. Allison, and J.F. Annett, Phys. Rev. Lett. **66**, 492 (1991).
[45] C. Enkvist, S. Lunell, B. Sjögren, P.A. Brühwiler, and S. Svensson, J. Chem. Phys. **103**, 6333 (1995).
[46] P.M.T.M. van Attekum and G.K. Wertheim, Phys. Rev. Lett. **43**, 1896 (1979).
[47] E.J. Mele and J.J. Ritsko, Phys. Rev. Lett. **43**, 68 (1979).
[48] P.A. Brühwiler, A.J. Maxwell, C. Puglia, A. Nilsson, S. Andersson, and N. Mårtensson, Phys. Rev. Lett. **74**, 614 (1995).
[49] R. Ahuja, P.A. Brühwiler, J.M. Wills, B. Johansson, N. Mårtensson, and O. Eriksson, Phys. Rev. B **54**, 14 396 (1996).
[50] J.J. Ritsko, Phys. Rev. B **25**, 6452 (1982).
[51] W. Schülke, A. Berthold, A. Kaprolat, and H.-J. Güntherodt, Phys. Rev. Lett. **60**, 2217 (1988).
[52] F. Sette, G.K. Wertheim, Y. Ma, G. Meigs, S. Modesti, and C.T. Chen, Phys. Rev. B **41**, 9766 (1990).
[53] C. Pisani, R. Dovesi, and P. Carosso, Phys. Rev. B **20**, 5345 (1979).
[54] E. Rotenberg, C. Enkvist, P.A. Brühwiler, A.J. Maxwell, and N. Mårtensson, Phys. Rev. B **54**, R5279 (1996).
[55] J. van den Brink and G. A. Sawatzky (unpublished).
[56] A.J. Maxwell, P.A. Brühwiler, D. Arvanitis, J. Hasselström, M.K.-J. Johansson, and N. Mårtensson, Phys. Rev. B **57**, 7312 (1998) (see Fig. 16).
[57] When analyzing the intensities from the different components one should also consider possible effects due to forward scattering. We recorded a set of angle-resolved spectra also for the (2×2) phase, not shown here, and we find no evidence that forward scattering effects are present in these spectra.
[58] A. Hohlfeld and K. Horn, Surf. Sci. **211/212**, 844 (1989).